Polymer Bulletin (2023) 80:3819–3841
https://doi.org/10.1007/s00289-022-04218-x

ORIGINAL PAPER

Octenyl succinate acidolysis carboxymethyl sesbania gum with high esterification degree: preparation, characterization and performance

Hongbo Tang[1] · Yihan Liu[1] · Yanping Li[1] · Xiaojun Liu[1]

Received: 6 August 2021 / Revised: 5 March 2022 / Accepted: 27 March 2022 /
Published online: 18 April 2022

Abstract

High esterification of acidolysis carboxymethyl sesbania gum was successfully accomplished by using 1-butyl-3-methylimidazolium chloride (ionic liquid) as a solvent, octenyl succinic anhydride as an esterifying agent, pyridine as a catalyst. The goal derivatives were characterized by FT-IR, TGA, SEM, XRD and so on. The experimental results indicated that octenyl succinate acidolysis carboxymethyl sesbania gum as a novel hydrophobic material had a very well emulsifying capacity (79.5%) and stability (78.9%). The effect of acidolysis on the crystalline structure of sesbania gum (SG) was different from the carboxymethylation. The esterification entirely destroyed the crystalline structure. The surface of SG particles would become rougher and rougher with the successive completion of carboxymethylation, acidolysis and esterification. The energy storage modulus of SG and SG derivatives increased with the increase in angular frequency, but the energy storage modulus of carboxymethyl sesbania gum increased in a different way. The peaks of C=O and C=C bonds appeared at 1735.0 cm^{-1} and 1630.0 cm^{-1} due to introduction of the carboxymethyl and octenyl succinate groups into SG molecular chains. Not only does SG show excellent performance in promoting the hydrophilicity and permeability due to containing large amounts of hydroxide radicals, but also SG is nontoxic and biodegradable.

Keywords Sesbania gum · Carboxymethylation · Esterification · Acidolysis · Structure · Property

✉ Hongbo Tang
tanghb6666@sina.com

[1] School of Environmental and Chemical Engineering, Shenyang University of Technology, Shenyang 110870, China

Introduction

Sesbania gum (SG) is one of the most commonly used plant polysaccharides, which have been employed widely in food, medicine and other fields owing to their thickening, binding, stabilizing and gelling performances [1–3]. The molecular weight of SG is about 500,000 g/mol [4]. Due to its similar chemical structure and physicochemical properties to guar gum and low cost, it is often viewed as a substitute for guar gum in many fields [5]. SG originates from the seed endosperm of sesbania grandiflora grown in the low latitude tropics. SG is soluble in water, but insoluble in organic solvents [6]. It is composed of β (1–4) glycosidic linkage to mannose and α (1–6) glycosidic linkage to galactose, and the molar ratio of galactose to mannose is 1:2 [7]. Although SG has some advantages of being environment-friendly, non-toxic and readily degradable, it cannot well meet the practical applications due to some weak points, such as the high content of water-insoluble substances, strong hydrophilicity, poor viscosity stability and long decomposition process with the more and more application requirements [8, 9]. The improvement of functional characteristics for some polymers can be realized effectively by the chemical modifications, such as the oxidation [10], cross-linking [11], hydroxypropylation [12], esterification [13], etherification [14] and so on. SG is also chemically modified like guar gum, cellulose and starch in order to make full use of its basic skeleton and retain some of its original basic performances. The carboxymethylation, which belongs to an etherification, is one of the most common chemical modifications at present. It can introduce the carboxymethyl groups into the molecular chains of the polymers by the hydroxyl groups in polymer reacting with monochloroacetic acid or monochloroacetic acid sodium [15]. The carboxymethylation is able to enhance the viscosity and water solubility of natural polymers such as starch and tara gum, and insert the electric charges into the molecular chains [16, 17].

The acidolysis is usually used for the modification of natural polymers in order to mainly reduce their viscosity through cleaving the long molecular chains into the short molecular chains. Although the acidolysis in the cutting chain is similar to the enzymolysis, the acidolysis is stochastic, whereas the enzymolysis is highly selective.

The esterification is also one of the most common modifications. According to the requirements of the different performances, however, the esterification of natural polymers such as guar gum, cellulose and starch is achieved selecting acetic anhydride, octenyl succinic anhydride, maleic anhydride and sodium metaphosphate as the esterifying agents. The esterification of octenyl succinic anhydride (OSA) chiefly improves the hydrophobicity of modified polysaccharides by means of the introduction of octenyl succinate groups into the corresponding molecular chains. Consequently, the natural polysaccharides esterified by OSA have become increasingly popular because of their low price, good hydrophobicity and strong emulsifying capacity [18], and have been applied in various fields for more than semi-centuries [19].

At present, SG is modified by oxidization [20], phosphorylation [21], carboxymethylation [22, 23], graft [24], hydroxypropylation, cross-linking [25] and so

on, while its esterification of OSA is not reported. The high degree of modification of polysaccharides usually needs to be accomplished in organic solvent or ionic liquid. Due to their unique characteristics such as low vapor pressure, non-combustibility, high chemical stability and good thermal stability, the ionic liquids as green solvents are selected by many researchers to prepare starch-based materials with high substitution degree or others instead of organic solvent, although the cost of ionic liquids is higher than that of organic solvent. Furthermore, the recovery of ionic liquid will also reduce its use cost.

The main goal of this work was to reasonably tailor SG functionalities by means of the combination modifications consisting of carboxymethylation, acidolysis and OSA esterification to prepare octenyl succinate acidolysis carboxymethyl sesbania gum (OSA-ACMSG) with the high emulsifying capacity and good thickening performances. On this basis, the influence of the carboxymethylation, acidolysis and esterification on the structure and properties of SG was investigated by infrared spectrometer, SEM, X-ray diffractometer, laser particle size meter, differential thermal analyzer and so on. The first attempt was made to perform high esterification of acidolysis carboxymethyl sesbania gum in an ionic liquid (1-butyl-3-methylimidazolium chloride) to achieve the high hydrophobicity of OSA-ACMSG. Compared with organic solvents, the advantages of ionic liquids were that the reaction time would be greatly shortened and the reaction efficiency was high in addition to unique characteristics. However, the cost of preparing OSA-ACMSG with high substitution degree was higher that of preparing OSA-ACMSG with low substitution degree or products obtained by other methods.

Materials and methods

Materials

Sesbania gum (SG, the size of SG particles ranged from about 8 μm to 295 μm, and its average size was 69.1 μm. The specific surface area of SG was 342.1 m^2/kg. The viscosity of SG aqueous solution was 1092.0 mPa s at a mass concentration of 2.0%) was provided by Xiangshui Unified Guar Gum Co. Ltd (China). Sodium hydroxide, chloroacetic acid, 1-butyl-3-methylimidazolium chloride (ionic liquid), pyridine, octenyl succinic anhydride (OSA), hydrochloric acid and ethyl alcohol were analytic grade.

Preparation of CMSG and OSA-ACMSG

30.0% (w/w) suspension was produced by mixing 10.0 g of dried SG (water contents = 9.81%) with 95.0% (w/w) ethanol solutions in a three-necked flask equipped with an electric mixer and a reflux device, stirred, heated to 35.0 °C in a water bath. 10.0 mL 5.0 mol/L sodium hydroxide aqueous solutions were added into the suspension. After the alkalization for 1.0 h, 0.3 g of chloroacetic acid was added into the suspension and the carboxymethylation was carried out for 4.0 h. The mixture

was treated by filtering, washing with 50.0% ethanol solutions three times, drying, smashing and sieving by 80 meshes in order to obtain carboxymethyl sesbania gum (CMSG, carboxyl contents = 1.13%) [26].

Since its high viscosity was not beneficial to the dissolution in following ionic liquids, CMSG needed to be partially hydrolyzed by acid to reduce its viscosity. 10.0 g of dried CMSG (water contents = 5.30%, carboxyl contents = 1.13%) was blended with 95.0% (w/w) of ethanol solutions in a three-necked flask to form a mixture with a mass concentration of 30%, stirred and heated to 45.0 °C in a water bath. After that, 30.0 mL 6.0 mol/L HCl was put into the flask, and the acidolysis was allowed to proceed for 4.0 h. Finally, the mixture was treated as the above-mentioned operation to obtain acidolysis carboxymethyl sesbania gum (ACMSG) with the fluidity of 89.0 mL (The fluidity of ACMSG was determined at a mass concentration of 5.0%) [27].

3 g of dried ACMSG (fluidity = 89.0 mL, carboxyl contents = 1.13%) was blended with a certain ionic liquid in a ratio of 1:14 in a three-necked flask. The mixture was heated to 120.0 °C in the oil bath and stirred for 30 min. 7.5 g of OSA (The mass ratio of OSA to dry ACMSG was 1:2.5) was added into the mixture after the ACMSG was completely dissolved in the ionic liquid. After that, 0.6 mL of pyridine as an organic base catalyst (The amount of pyridine added was 0.2 mL per gram of dried ACMSG) was added into the mixture, and the esterification was conducted for 90.0 min. The crude product was precipitated with 250.0 mL of 60.0% ethanol solutions and then filtered, washed with 50.0% ethanol solutions four times, dried and smashed. Finally, octenyl succinate acidolysis carboxymethyl sesbania gum (OSA-ACMSG) with high substitution degree was obtained [28]. The schematic diagram of carboxymethylation, acidolysis and OSA esterification was as follows:

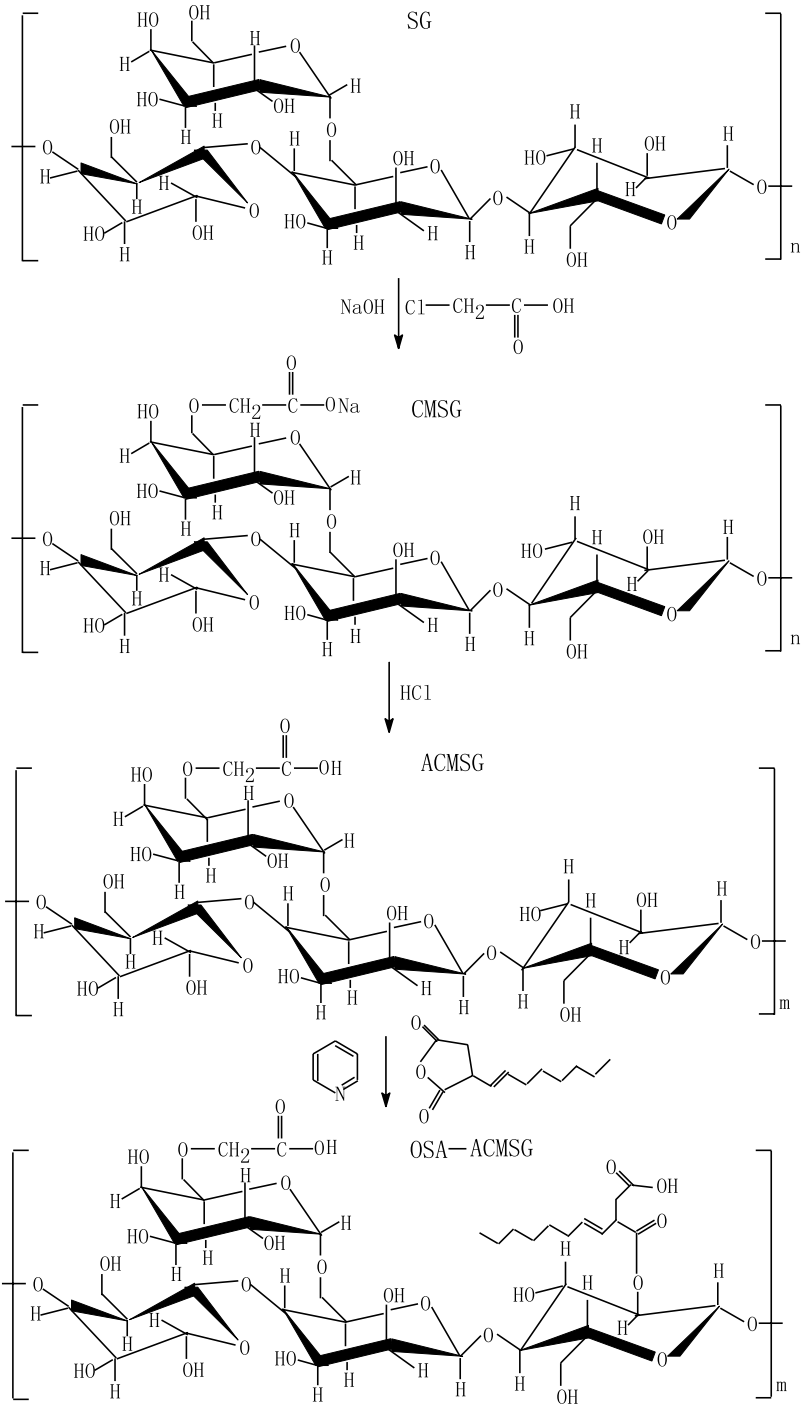
SG
NaOH
Cl—CH2—C—OH
O
CMSG
HCl
ACMSG
OSA—ACMSG

Determination of carboxyl content, degree of substitution (DS) and acidolysis degree

The degree of carboxymethyl etherification was measured with the carboxyl content, which was determined by a previously published method [29]. 1.0 g of dried CMSG was placed in a 100.0 mL flask. The powders were first wetted with a few drops of ethanol, subsequently mixed with 25.0 mL of 0.1 mol/L HCl, and kept stirring for 30 min. After that, the suspension was filtered by a vacuum. The obtained cake was washed with 60.0% (w/w) ethanol solution until chloride ions in the cake were totally removed. At last, the filter cake was placed in a conical flask with 300.0 mL distilled water and a few drops of phenolphthalein, and the mixture was titrated with 0.1 mol/L NaOH to the terminal point. The content of carboxyl groups was calculated using Eq. (1).

$$\mathrm{COOH} = \frac{(V_1 - V_0) \times 0.045 \times 0.1}{m} \times 100\% \tag{1}$$

where V_1 and V_0 are the volume of 0.1 mol/L NaOH solution consumed for the sample and blank (mL), respectively. The m is the mass of samples (g).

The degree of substitution (DS) was defined as the average numbers of hydroxyl groups substituted per glucose unit. The degree of esterification was measured with degree of substitution and determined by a previously published method [30]. 0.5 g of sample (dry base) and 10 mL of 75.0% (w/w) ethanol solution were placed in a 100.0 mL iodine flask, and then 10.0 mL of 0.5 mol/L NaOH and a few drops of phenolphthalein were added into this flask for saponification and titration. At this time, the color of paste would be immediately transformed into a pink. The paste was wobbled for 5.0 h at 50.0 °C after the iodine flask was covered by lid. Next, the lid and neck of the flask were washed with a little distilled water, and then the mixture was titrated with 0.5 mol/L HCl until its pink disappeared. 10.0 mL 0.5 mol/L NaOH was titrated as blank. The degree of substitution (DS) was calculated using following Eq. (2) and Eq. (3).

$$W_{\mathrm{MA}} = \frac{210 \times 0.5 \times (V_1 - V_2)}{1000 \times 2W} \times 100\% \tag{2}$$

$$\mathrm{DS} = \frac{162 \times W_{\mathrm{MA}}}{210 \times \left(100 - W_{\mathrm{MA}}\right)} \tag{3}$$

where the V_1 and V_2 are the volume of 0.5 mol/L HCl consumed by sample and blank (mL), respectively. The W represents the sample mass (g), the W_{MA} represents the content of octenyl succinate groups (%).

The degree of acidolysis of CMSG and ACMSG was evaluated with the fluidity [31].

Determination of freeze–thaw stability, swelling power, acid and alkali resistance

The freeze–thaw stability, swelling capacity, acid and alkali resistance were determined by previously published literature [32–35]. The freeze–thaw stability of samples was evaluated by measuring the syneresis rate for five times at a mass concentration of 1.0% (w/w). The freezing conditions were: temperature of − 18 °C, freezing time of 24 h at every turn. The swelling power was measured at a mass concentration of 1.5% (w/w), temperature of 80 °C, and the corresponding formula was as follows:

$$S = \frac{m_A}{m_S} \times 100 \tag{4}$$

$$\text{Swelling power } (\%) = \frac{m_P \times 100}{m_S(100 - S)} \tag{5}$$

Here, S is the solubility (%), m_{A} is the mass of dried residue of supernatant (g), m_{P} is the mass of sediment paste (g), m_{S} is mass of dry sample (g).

The acid and alkaline resistance of samples was evaluated by the viscosity change rate at the pH of 3 and 10, respectively. The corresponding measurement conditions were: temperature of 25 °C, mass concentration of 2.0% (w/w). The viscosity was completed by an NDJ-8S rotary viscometer (Shenzhen Lida Xinyi Instrument Co. LTD., China).

Determination of particle size distribution and hydrophobicity

The size distribution of SG and SG derivative granules was determined by a MASTERSIZER3000 (Malvern, UK) [36].

The hydrophobicity of SG and SG derivatives was evaluated by the contact angle. If the contact angle < 90.0°, the solid surface was hydrophilic; if the contact angle > 90.0°, the solid surface was hydrophobic. The samples were pressed into a slice to measure their contact angle with water. The slice was placed on the glass slide and moved the glass slide to the center of lens. The micro-syringe was slowly descended until the water drops contacted with the slice, and then the micro-syringe was raised rapidly. Finally, the water droplets were left on the solid surface to take photographs, and the contact angle was determined using the five-point fitting method [37].

Fourier transform infrared (FT-IR), rheology, X-ray diffraction (XRD), scanning electron microscope (SEM) and thermogravimetric analysis (TGA)

FT-IR spectra of samples were recorded using an IR Prestige-21 infrared spectrometer (Shimadzu Corporation, Japan) within the range of 4000–400 cm^{-1} [38, 39]. The rheological characteristics of samples were measured using a MCR102 rheometer in

the modes (ACMSG and OSA-ACMSG based on first mode, SG and CMSG based on second mode. First mode: low viscosity fluid, temperature of 25.0 °C, the gap 0.5 mm, initial shearing rate 1.0 s^{-1}, final shearing rate 100.0 s^{-1}; Second mode: viscoelastic fluid, temperature of 25.0 °C, the gap 1.0 mm, initial shearing rate 0.1 s^{-1}, final shearing rate 100.0 s^{-1}) [40, 41]. XRD patterns were obtained using a Bruker D8 ADVANCE X-ray diffractometer (Bruker AXS GmbH, Germany) in the reflection mode (The angle range from 10.0 to 90.0°, steps of 0.03°) [42, 43]. The particle morphology was observed by a Hitachi S-3400 N scanning electron microscope (Hitachi Inspire the Next, Japan) [44–46]. The TGA curves of samples were determined by a *Q* 50 V 20.10 Build 36 thermogravimetric analyzer (TA Instruments, US) within the temperature range of 20.0–600.0 °C at a heating rate of 10.0 °C/min [47].

Determination of emulsifying capacity and stability

The paste was prepared by blending 0.5 g dried samples with 35.0 g distilled water in a 100.0 mL beaker, and heated in a water bath until the paste was entirely uniform, and then cooled to the room temperature. After that, 15.0 g salad oil was added into the paste, and the mixture was homogenized by an IKA Color Squid White magnetic mixer at 1500 r/min for 30.0 min. Four 10.0 mL mixtures were taken and placed into four 10 mL graduated centrifuge tubes, respectively, and centrifuged at 3000 r/min for 15.0 min. The emulsifying layer height (H_0) and total liquid height (H) were recorded, and the emulsifying capacity (EC) was calculated by following formula. The results were averaged.

$$\mathrm{EA} = \frac{H_0}{H} \times 100\% \tag{6}$$

The emulsifying stability of samples was determined by same operations as above. Four 10.0 mL homogenized mixtures were taken and placed into four 10.0 mL graduated centrifuge tubes, respectively. After standing for 24.0 h, these centrifuge tubes were centrifuged at 3000 r/min for 15.0 min. The corresponding emulsification layer height (H_0) and total liquid height (H) were recorded, and the emulsifying stability (ES) was calculated by following formula [48].

$$\mathrm{ES} = \frac{H_0}{H} \times 100\% \tag{7}$$

Determination of potato starch gelatinization characteristics

The gelatinization characteristics of potato starch and potato starch containing SG or its derivatives were measured by a MCR102 rheometer (Anton Paar, Austria). The mass concentration of potato starch and potato starch containing SG or its derivatives was 5.0% (w/w), and the amount of adding SG or its derivatives was 0.2% (the mass percentage ratio of SG or its derivatives to dry potato starch). Measuring

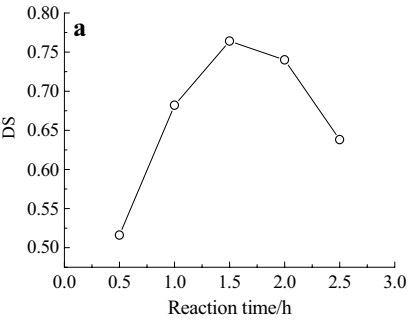

Reaction conditions: reaction temperature 120.0 °C, amount of OSA 250.0 %, amount of pyridine 30.0 %, amount of ionic liquid 1400.0 %.

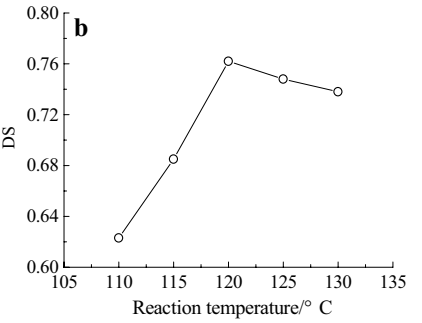

Reaction conditions: reaction time 1.5 h, amount of OSA 250.0 %, amount of pyridine 30.0 %, amount of ionic liquid 1400.0 %.

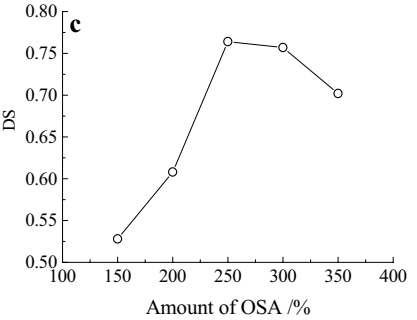

Reaction conditions: reaction time 1.5 h, reaction temperature 120.0 °C, amount of pyridine 30.0 %, amount of ionic liquid 1400.0 %.

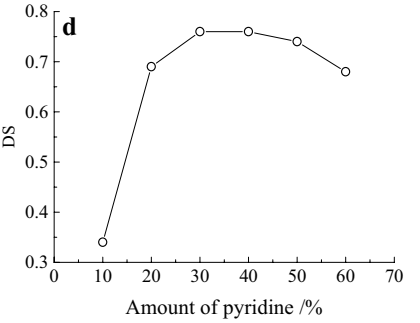

Reaction conditions: reaction time 1.5 h, reaction temperature 120.0 ° C, amount of OSA 250.0 %, amount of ionic liquid 1400.0 %.

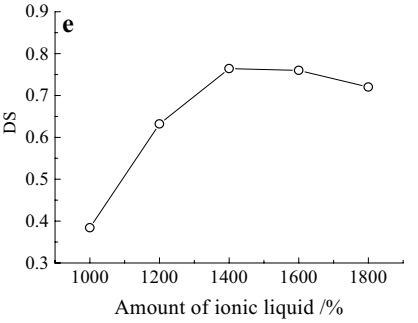

Reaction conditions: reaction time 1.5 h, reaction temperature 120.0 °C, amount of pyridine 30.0 %, amount of OSA 250.0 %.

Fig. 1 Effect of esterification conditions on DS of OSA-ACMSG

conditions: held at 50.0 °C for 1 min, heated to 95.0 °C at 6.0 °C/min, held at 95.0 °C for 5.0 min, cooled down to 50.0 °C at 6.0 °C/min, held at 50.0 °C for 2.0 min [49].

Results and discussion

Effect of esterification conditions on DS of OSA-ACMSG.

The effect of esterification conditions, such as reaction time, reaction temperature, amount of OSA, amount of pyridine and amount of ionic liquid, on the DS of OSA-ACMSG is presented in Fig. 1. Here, ACMSG (dry, fluidity = 89.0 mL, carboxyl contents = 1.13%) was held at 1.3 g during the esterification. The amount of OSA, pyridine and ionic liquid was defined as the mass percentage ratio of OSA, pyridine and ionic liquid to dry ACMSG, respectively. From Fig. 1a, the DS of OSA-ACMSG was increased with the increase in reaction time when it was below 1.5 h. When the reaction time exceeded 1.5 h, however, the DS of OSA-ACMSG decreased. This phenomenon can be explained as follows: Since the alkaline environment generated by pyridine as a catalyst was favorable for the esterification to proceed in opposite direction under a long time, the DS of OSA-ACMSG was reduced. In fact, the reaction time of 1.5 h was much less than that reported in the literature [50].

From Fig. 1b, the effect of the reaction temperature on DS of OSA-ACMSG increased first and then decreased from 110.0 to 130.0 °C, and the DS reached a maximum value of 0.76 at 120.0 °C. The result was consistent with the esterification temperature of starch laurate reported in reference [51]. When the reaction temperature was above 120.0 °C, the increase in the reaction temperature was unfavorable to the esterification. It should associate with the increase in the side reactions caused by high temperature.

From Fig. 1c, the effect of amount of OSA on DS of OSA-ACMSG was similar to that of reaction temperature. The DS had an optimum value when the amount of OSA was from 150.0 to 350.0%. The reduction in DS should be related to the growth of the side reaction, namely a part of OSA was converted to salt so that the esterification efficiency decreased.

Pyridine acted as a catalyst during the esterification [52]. The effect of pyridine on the reaction could be clearly seen from Fig. 1d. A small amount of pyridine could greatly enhance the efficiency of esterification, while a large amount of pyridine caused a slight reduction in the DS. This should be that the more pyridine hindered the contact between OSA and SG. During the esterification, furthermore, the DS

Table 1 Freeze–thaw stability, swelling power, acid and alkali resistance of SG, CMSG, ACMSG and OSA-ACMSG

Samples	SG	CMSG	ACMSG	OSA-ACMSG
Syneresis rate/%	75.2	67.9	36.2	16.0
Swelling power/%	15.8	17.6	3.9	1.3
Viscosity/mPa s	1092.0	1082.0	17.5	8.9
Viscosity (pH = 3)/mPa s	958.0	934.0	12.3	8.3
Variation rate of viscosity (pH = 3)/%	12.2	22.7	29.7	6.7
Viscosity (pH = 10)/mPa s	1407.0	1806.0	19.8	10.0
Variation rate of viscosity (pH = 10)/%	28.9	49.5	13.1	12.4

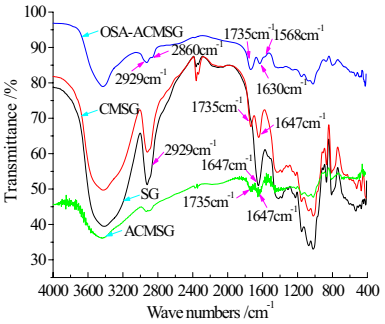

Fig. 2 FTIR of SG, CMSG, ACMSG and OSA-ACMSG

of OSA-ACMSG could reach a value of 0.76 at the amount of pyridine of 30.0%. Therefore, according to the variation tendency of the curve, the required amount of pyridine was not less than 20.0% to obtain OSA-ACMSG with high DS.

From Fig. 1e, the influence of ionic liquid on the esterification was similar to that of reaction time. The low amount of ionic liquid could lead to more ACMSG to be insoluble so that the DS was reduced, whereas an excess of ionic liquid diluted the concentration of OSA in this system so that it slightly influenced the contact between OSA and ACMSG.

Above all, the suitable esterification conditions were as follows: reaction temperature 120.0 °C, reaction time 1.5 h, amount of OSA 250.0%, amount of pyridine 30% and amount of ionic liquid 1400.0%.

Effect of carboxymethylation, acidolysis and esterification on freeze–thaw stability, swelling power, acid and alkali resistance.

The freeze–thaw stability, swelling capacity, acid and alkali resistance of SG, CMSG (carboxyl contents = 1.13%, the same below), ACMSG (carboxyl contents = 1.13%, fluidity = 89.0 mL, the same below) and OSA-ACMSG (carboxyl

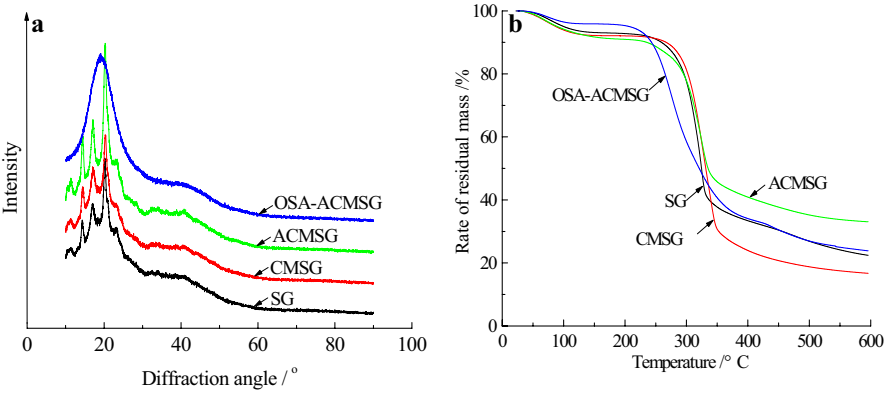

Fig. 3 XRD **a** and TGA **b** cureves of SG, CMSG, ACMSG and OSA-ACMSG

contents = 1.13%, fluidity = 89.0 mL, DS = 0.76, the same below) are shown in Table 1. As far as the frozen products were concerned, the freeze–thaw stability of SG and SG derivatives was very important to guarantee the quality of the products added by SG or SG derivatives during the freezing storage process. After the carboxymethylation, acidolysis and esterification of SG, the syneresis rate of SG derivatives was evidently less than that of SG. The syneresis rate of OSA-ACMSG was the lowest, indicating that the freeze–thaw of OSA-ACMSG was the best among these derivatives, and OSA-ACMSG could be used well for the frozen products in this regard. The swelling capacity of SG derivatives was less than that of SG except for CMSG. Interestingly, the viscosity of SG, CMSG and OSA-ACMSG all decreased when the pH of their paste was 3.0, while the viscosity of SG, CMSG and OSA-ACMSG all increased at the pH of 10.0. Furthermore, according to the variation rate of the viscosity, we could obtain that the acid resistance was in order of OSA-ACMSG > SG > CMSG > ACMSG, and the alkali resistance was in order of OSA-ACMSG > ACMSG > SG > CMSG.

Analysis of Fourier transform infrared (FT-IR), X- ray diffraction (XRD), TGA, size distribution and particle morphology

The FT-IR of SG and SG derivatives are shown in Fig. 2. The FT-IR of CMSG, ACMSG and OSA-ACMSG were clearly dissimilar to that of SG. A new peak at 1735.0 cm^{-1} which belonged to the stretching vibration of the C=O bonds appeared on CMSG, ACMSG and OSA-ACMSG FT-IR curves. The difference was that the peak intensity of the C=O bonds was different on these curves. The similar results about the peak position of the C=O bonds were also reported in the literature [53]. It confirmed that SG was successfully etherified by chloroacetic acid, and the carboxymethyl groups in CMSG, ACMSG were also influenced by the esterification. Moreover, the discernible peaks at 1148.0 cm^{-1} were attributed to the asymmetric stretching vibration of C–O–C bonds and confirmed that the carboxymethylation, acidolysis and esterification did not destroy the basic structure of SG. However, the stretching vibration peak of C–H bond in OSA-ACMSG FT-IR was also different from others. Due to the influence of the high contents of octenyl succinate groups, it was split into two peaks at the wave numbers of 2929.0 cm^{-1}, 2860.0 cm^{-1}, separately. The occurrence of two peaks should be

Table 2 The key groups and position of corresponding peaks

Groups	Wave numbers/cm^{-1}
C=O	1735.0
C–O–C	1148.0
C–H in methyl groups	2929.0
C–H in methylene groups	2860.0
H–O–H	1647.0
C=C	1630.0
$RCOO^-$	1568.0

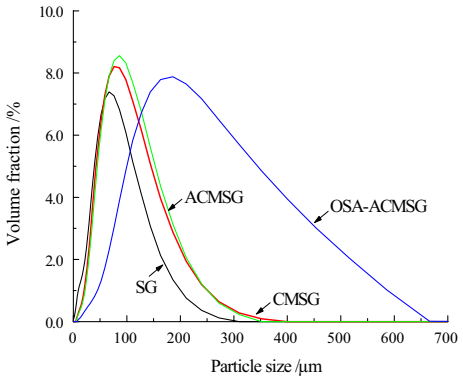

Fig. 4 Sixe distribution of SG and its derivatives

Table 3 The TGA thermodynamics data of SG, CMSG, ACMSG and OSA-ACMSG

Samples	SG	CMSG	ACMSG	OSA-ACMSG
Onset decomposition temperature/°C	282.4	294.6	290.0	243.7
End decomposition temperature/°C	332.1	353.7	341.2	324.5
Weight loss rate/%	44.0	54.1	34.2	41.2

attributed to the methyl and methylene C–H stretching associated with the octenyl substituents [54]. Another typical peak at 1647.0 cm^{-1} only in SG, CMSG and ACMSG FT-IR was attributed to the bending vibration of H–O–H bonds, but the peak of H–O–H bonds on OSA-ACMSG disappeared. It confirmed that water adsorbed by OSA-ACMSG was much smaller that adsorbed by SG, CMSG and ACMSG, that is, the hydrophobicity of OSA-ACMSG was much stronger than that of SG, CMSG and ACMSG. In addition, a new peak at 1630.0 cm^{-1} revealed the stretching vibration of C=C bonds. A new small peak at 1568.0 cm^{-1} revealed the asymmetric stretching vibration of carboxylate $RCOO^{-}$. It indicated that the octenyl succinate groups were successfully introduced into OSA-ACMSG. The result was also consistent with the result provided in the literature [55]. Finally, the peaks of the above key groups are listed in Table 2 to clearly identify them.

From Fig. 3a, any new peak was not introduced into XRD patterns of CMSG, ACMSG, compared with SG. The diffraction peaks of SG, CMSG and ACMSG appeared at the diffraction angle of 11.4°, 14.5°, 17.1°, 20.3° and 23.2°, respectively. The carboxymethylation and acidolysis only changed the peak intensity. The carboxymethylation weakened the peak intensity at 20.3°, while the acidolysis strengthened the peak intensity. Moreover, the acidolysis also enhanced the peak intensity at the diffraction angle of 14.5°, 17.1° and 20.3°. However, the above-mentioned peaks of OSA-ACMSG vanished. Therefore, it confirmed that SG, CMSG and ACMSG were a semicrystalline polymer, but OSA-ACMSG became an amorphous polymer, namely the esterification changed the crystalline structure of SG. The amorphous structure of OSA-ACMSG should be caused by the esterification completed in ionic liquid. However, the semicrystalline structure of SG

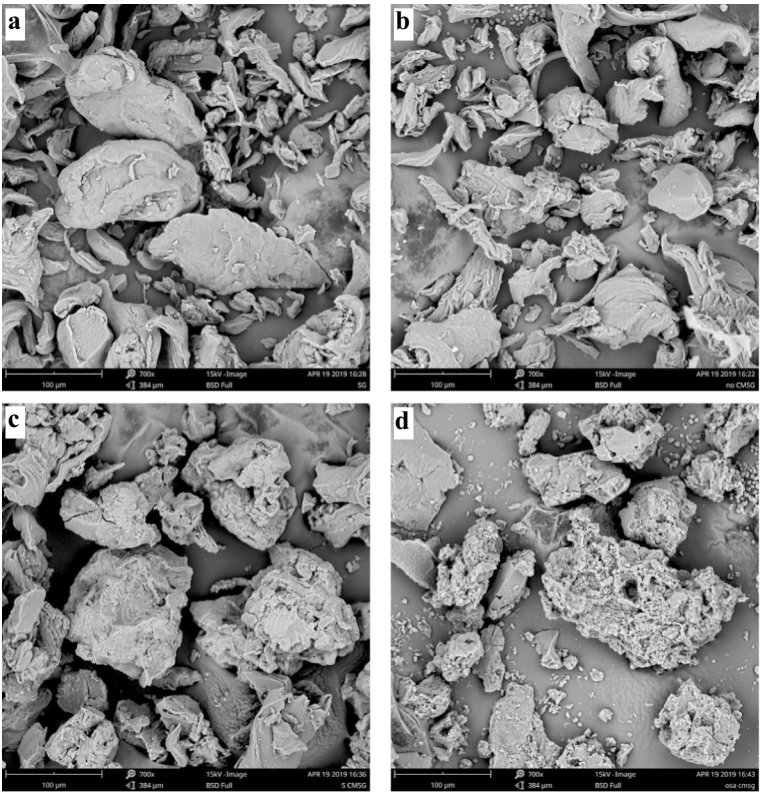

Fig. 5 SEM photos of SF (**A**), CMSG (**B**), ACMSG (**C**) and OSA-ACMSG (**D**)

Table 4 Key parameters of size distribution of SG and its derivative particles

Samples	Specific surface area m^2/kg	Dx (10)/μm	Dx (50)/μm	Dx (90)/μm
SG	342.1	13.0	60.8	134.0
CMSG	100.8	33.3	80.3	169.0
ACMSG	94.6	36.0	84.5	171.0
OSA-ACMSG	46.1	73.1	185.0	400.0

was different from that reported in the literature [26]. Eventually, the crystallinity degrees of SG, CMSG and ACMSG were calculated using MIDI jade 6.0 Software as 56.2%, 51.4% and 69.0%, respectively. It was clearly proved that the carboxymethylation destroyed the crystalline region, but the acidolysis destroyed the amorphous region.

From Fig. 3b, TGA curves of SG, CMSG, ACMSG and OSA-ACMSG consisted of dehydration and decomposition which was composed of rapid decomposition and slow decomposition stages. The decomposition of polymers was

related to their composition, chain size and structure. The TGA curve of SG was influenced by the carboxymethylation, acidolysis and esterification. The carboxymethylation and esterification significantly lowered the residual amount of decomposition products, similar results were reported by others [56, 57]. However, the acidolysis obviously increased the residual amount of decomposition products. The esterification slowed down the rapid decomposition stage. Moreover, the TGA thermodynamics data of SG, CMSG, ACMSG and OSA-ACMSG were calculated and are listed in Table 3 to further analyze the effect of acidolysis, carboxymethylation and esterification on the thermal properties of SG. From Table 3, the carboxymethylation increased the onset decomposition temperature and end decomposition temperature, whereas the esterification and acidolysis decreased the onset decomposition temperature and end decomposition temperature. The sequence of the thermal stability was in order of ACMSG > OSA-ACMSG > SG > CMSG.

From Fig. 4 and Table 4, it could be seen that the particle size distribution of CMSG, ACMSG and OSA-ACMSG was more than that of SG. The carboxymethylation and esterification increased the average particle size of SG more than the acid hydrolysis. Especially, the Dx [50] and Dx [90] of OSA-ACMSG could reach 185.0 μm and 400.0 μm, respectively, and were much larger than those of SG. At the

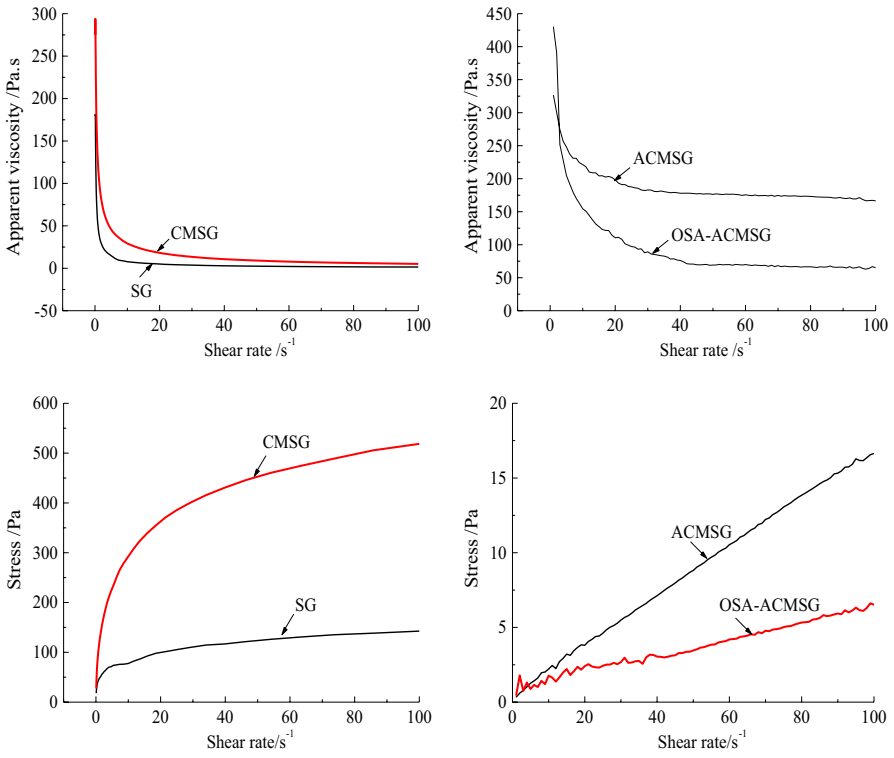

Fig. 6 Static rheological curves of SG, CMSG, ACMSG, and OSA-ACMSG

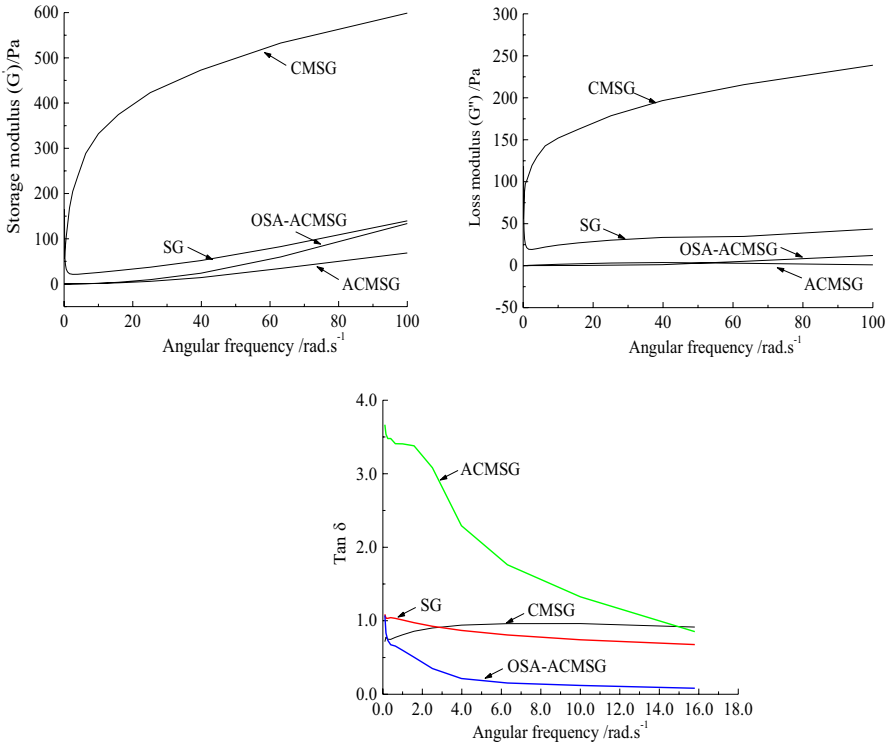

Fig. 7 Dynamic rheological curves of SG, CMSG, ACMSG, and OSA-ACMSG

same time, the specific surface area of SG decreased as deepening the modification degree. The reduction of SG derivatives in specific surface area also indirectly confirmed that CMSG, ACMSG and OSA-ACMSG particles experienced the inflation during the modification.

The scanning electron microscope (SEM) photographs of SG, CMSG, ACMSG and OSA-ACMSG are shown in Fig. 5. From Fig. 5, the particles of CMSG, ACMSG and OSA-ACMSG were evidently different from those of SG. The surface of SG particles was smooth, and their shape was irregular, and their size was very uneven. After the carboxymethylation, acidolysis and esterification of SG, the surface of CMSG, ACMSG and OSA-ACMSG became rough and further deteriorated as increasing the modification degree. Interestingly, the carboxymethylation created the deep grooves on CMSG grains, whereas the acidolysis made the grooves disappear. The honeycomb holes appeared on OSA-ACMSG grains. This should be caused by the recrystallization during the homogeneous synthesis of OSA-ACMSG. Therefore, we could conclude that the carboxymethylation and acidolysis had different destructive ways upon the modification of SG.

Table 5 Contact angle of SG, CMSG, ACMSG and OSA-ACMSG

Samples	SG	CMSG	CMSG	ACMSG
Contact angle/°	85.5	84.0	84.6	98.8

Effect of carboxymethylation, acidolysis and esterification on hydrophobicity of SG

The effect of carboxymethylation, acidolysis and esterification on hydrophobicity of SG is shown in Table 5. As we know, if the contact angle of powders was greater than 90.0°, the powders were hydrophobic, and vice versa. From Table 5, the contact angle of SG, CMSG, ACMSG and OSA-ACMSG was 85.5°, 84.0°, 84.6° and 98.8°, respectively. Obviously, the carboxymethylation, acidolysis basically did not change the hydrophobicity of SG, but the OSA esterification enhanced its hydrophobicity. Namely, the SG, CMSG, ACMSG were still hydrophilic, while the OSA-ACMSG was hydrophobic. It further proved that the hydrophobic groups were successfully introduced into OSA-ACMSG molecular chains. The result was accordance with that obtained in the literature [58].

Effect of carboxymethylation, acidolysis and esterification on rheological properties of SG

The static and dynamic rheological curves of SG and SG derivatives are presented in Figs. 6 and 7. From Fig. 6, the apparent viscosity of SG and SG derivatives decreased with increasing the shearing rate, but the stress of SG and SG derivatives increased with increasing the shearing rate. The apparent viscosity of SG and CMSG descended more quickly than ACMSG and OSA-ACMSG. The change trend

Table 6 The emulsifying capacity and stability of SG, CMSG, ACMSG and OSA-ACMSG

Samples	SG	CMSG	ACMSG	OSA-ACMSG
Emulsifying capacity/%	2.4	28.6	8.4	79.5
Emulsifying stability/%	–	11.3	2.2	78.9

Table 7 Effect of adding SG, CMSG, ACMSG and OSA-ACMSG on key parameters of potato starch gelatinization characteristics

Samples	PT/°C	PV/cP	TV/cP	FV/cP	BD/cP	SB/cP
Potato starch	70.5	1126.0	903.0	1504.0	223.0	621.0
Potato starch added by 0.2% SG	69.0	2110.0	1152.0	1773.0	958.0	958.0
Potato starch added by 0.2% CMSG	68.7	1937.0	1140.0	1723.0	797.0	583.0
Potato starch added by 0.2% ACMSG	68.9	1780.0	1138.0	1781.0	642.0	643.0
Potato starch added by 0.2% OSA-ACMSG	69.3	2128.0	1152.0	1753.0	976.0	601.0

PT Pasting temperature, *PV* peak viscosity, *TV* trough viscosity, *BD* breakdown (BD = PV − TV), *FV* final viscosity, *SB* setback (SB = FV − TV)

in the stress of SG and CMSG was entirely different from that of ACMSG and OSA-ACMSG. The stress of latter two almost linearly increased as increasing the shearing rate.

The storage modulus (G'), loss modulus (G") and tan δ were used to measure the stored energy. G' and G" represented the ability to store elastic deformation energy, viscosity, respectively. The tan δ reflected the relative strength of elastic and viscous properties of samples. From Fig. 7, the energy storage modulus (G') of SG, CMSG, ACMSG and OSA-ACMSG increased with the increase in angular frequency, but the increase in CMSG in the energy storage modulus was different from that of SG, ACMSG and OSA-ACMSG. The loss modulus (G") of CMSG varied greatly with the increase in angular frequency, while the loss modulus (G") of SG, ACMSG and OSA-ACMSG varied little. For the tan δ, the trend of CMSG was also different from that of SG, ACMSG and OSA-ACMSG. The tan δ of SG, ACMSG and OSA-ACMSG decreased as increasing the angular frequency within a certain range, but the tan δ of CMSG increased with the angular frequency when the angular frequency was below 4.0 rad/s. The tan δ of OSA-ACMSG was the lowest among SG, CMSG and ACMSG when the angular frequency was greater than about 0.5 rad/s. The above results confirmed that SG, CMSG, ACMSG and OSA-ACMSG had the gel characteristics. And the carboxymethylation, acidolysis and esterification could have an influence on the elasticity and glutinosity of SG in different levels.

Emulsifying capacity and stability of SG and its derivatives

The emulsifying capacity and stability of SG, CMSG, ACMSG and OSA-ACMSG are presented in Table 6. From Table 6, the emulsifying capacity of SG was very poor, and the emulsifying capacity of OSA-ACMSG was the best. The carboxymethylation and esterification of OSA [59] could improve the emulsifying capacity of SG, but the effect of OSA esterification was much better than that of carboxymethylation. The acidolysis could not improve the emulsifying capacity of SG. This phenomenon might be from the production of many short hydrophilic chains due to the cleavage of chains by the acidolysis. In addition, the emulsifying stability of OSA-ACMSG was much stronger than that of CMSG. And the sequence of the emulsifying stability was in order of OSA-ACMSG, CMSG and SG.

Effect of adding SG and its derivatives on gelatinization characteristics of potato starch

The effects of adding SG and its derivatives on the gelatinization characteristics of potato starch are presented in Fig. 8 and Table 7. From Fig. 8, adding SG, CMSG, ACMSG and OSA-ACMSG obviously affected the gelatinization characteristics of potato starch. Adding SG or OSA-ACMSG made to the viscosity of the mixture paste more than 2000.0 cP at the amount of SG or OSA-ACMSG 0.2%. After adding SG, CMSG, ACMSG and OSA-ACMSG, the final viscosity of the mixture paste obviously increased. It would take different time for the mixture paste to reach

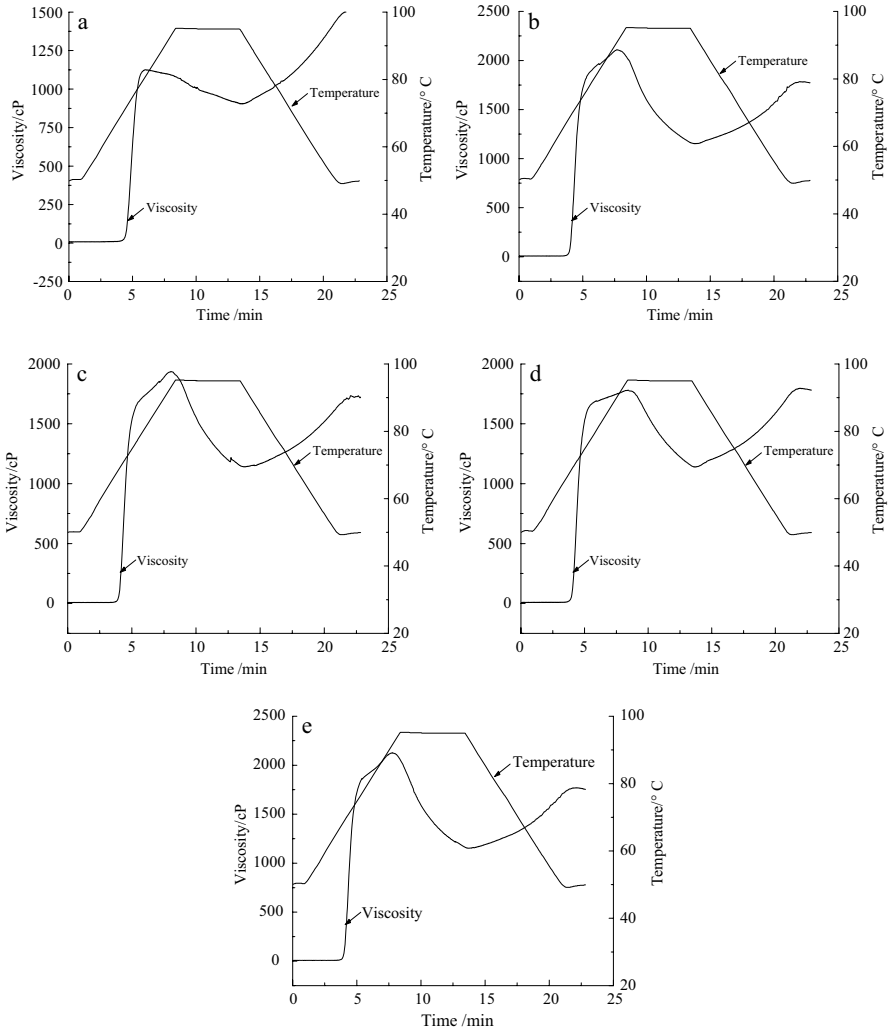

Fig. 8 Effect of adding SG, CMSG, ACMSG and OSA-ACMSG on pasting properties of potato starch. **a** Potato starch, **b** potato starch added by 0.2% SG, **c** potato starch added by 0.2% CMSG, **d** potato starch of 0.2% ACMSG, **e** potato starch of 0.2% OSA-ACMSG

the peak viscosity. Potato starch and potato starch mixed SG, CMSG, ACMSG and OSA-ACMSG took 8.07 min, 7.70 min, 8.03 min, 8.43 min and 7.80 min to reach peak viscosity, respectively.

From Table 7, after adding SG, CMSG, ACMSG and OSA-ACMSG, the pasting temperature of potato starch decreased, whereas its breakdown increased. The setback of potato starch added by CMSG or OSA-ACMSG was less than that of potato starch, but the setback of potato starch added by SG or ACMSG was greater than

that of potato starch. Moreover, adding SG, CMSG, ACMSG and OSA-ACMSG increased the peak viscosity and trough viscosity of potato starch.

Conclusions

The absorption peaks of C=O bonds at 1735.0 cm^{-1} and C=C bonds at 1630.0 cm^{-1} on CMSG and OSA-ACMSG FT-IR curves confirmed that the carboxymethyl and octenyl succinate groups were successfully inserted into the SG molecular chains. The carboxymethylation and OSA esterification could increase the emulsifying capacity and stability of SG, but the effect OSA esterification was much better than the carboxymethylation. The carboxymethylation could lead to the large swelling of SG particles, whereas the acidolysis could only result in the small expansion. CMSG was different from SG and other materials in increasing the storage modulus. The OSA esterification was able to ameliorate the acid and alkali resistance of SG. The destruction of SG particles by the acidolysis was different from the carboxymethylation. SG, CMSG, ACMSG and OSA-ACMSG had the gel characteristics. The addition of CMSG or OSA-ACMSG could lower the setback of potato starch. The addition of SG, CMSG, ACMSG and OSA-ACMSG would worsen the shearing resistance of potato starch. Finally, it could be concluded that SG derivatives could be used as gelling agent, thickener, adhesive and stabilizer for the medicine delivery and food emulsification in the future.

Acknowledgements We are grateful to people for our research support.

Declarations

Conflict of interest The manuscript was written through the contributions of all authors. All authors have given approval to the final version of the manuscript. All the authors declare no conflict of interest.

References

1. Prajapati VD, Jani GK, Moradiya NG, Randeria NP (2013) Pharmaceutical applications of various natural gums, mucilages and their modified forms. Carbohydr Polym 92:1685–1699
2. Patel GC, Patel MM (2009) Preliminary evaluation of sesbania seed gum mucilage as gelling agent. Int J PharmTech Res 1:840–843
3. Bharadia PD, Patel MM, Patel GC, Patel GN (2004) A preliminary investigation on sesbania gum as a pharmaceutical excipient. Int J Pharm Excip 4:99–102
4. Pal P, Banerjee A, Halder U, Pandey PJ, Sen G, Bandopadhyay R (2018) Conferring antibacterial properties on sesbania gum via microwave assisted graft copolymerization of DADMAC. J Polym Environ 26:3272–3282
5. Tang HB, Yao Y, Li YP, Dong SQ (2018) Effect of cross-linking and oxidization on structure and properties of sesbania gum. Int J Biol Macromol 114:640–648
6. Pal P, Pandey PJ, Sen G (2018) Grafted sesbania gum: a novel derivative for sugarcane juice clarification. Int J Biol Macromol 114:349–356

7. Zhang Q, Gao Y, Zhai YA, Liu FQ, Gao G (2008) Synthesis of sesbania gum supported dithiocarbamate chelating resin and studies on its adsorption performance for metal ions. Carbohydr Polym 73:359–363
8. Liu HJ, Qi RL, Gao L, Xue M, Shen D (2012) Grafting modification of sesbania gum and sizing performance. Adv Mater Res 424–425:1211–1214
9. Li R, Jia X, Wang YQ, Li Y, Cheng YQ (2019) The effects of extrusion processing on rheological and physicochemical properties of sesbania gum. Food Hydrocoll 90:35–40
10. Gong H, Liu M, Zhang B, Cui D, Gao C, Ni B, Chen J (2011) Synthesis of oxidized guar gum by dry method and its application in reactive dye printing. Int J Biol Macromol 49:1083–1091
11. Tanetrungroj Y, Prachayawarakorn J (2018) Effect of dual modification on properties of biodegradable crosslinked-oxidized starch and oxidized-crosslinked starch films. Int J Biol Macromol 120:1240–1246
12. Zhu J, Guo P, Chen D, Xu K, Wang P, Guan S (2017) Fast and excellent healing of hydroxypropyl guar gum/poly (*N*, *N*-dimethyl acrylamide) hydrogels. J Polym Sci Part B Polym Phys 56:239–247
13. Borah PK, Rappolt M, Duary RK, Sarkar A (2018) Effects of folic acid esterification on the hierarchical structure of amylopectin corn starch. Food Hydrocoll 86:162–171
14. Rekaby MM, Elthalouth IA, Rahman AAH, Elkhabery ES (2010) Technological evaluation of carboxymethyl sesbania galactomannan gum, derivatives as thickeners in reactive printing. BioResources 5:1517–1529
15. Wilpiszewska K (2019) Hydrophilic films based on starch and carboxymethyl starch. Pol J Chem Technol 21:26–30
16. Wu Z, Song X (2006) Carboxymethylation of γ-irradiated starch. J Appl Polym Sci 101:2210–2215
17. Santos MB, Santos CHD, Carvalho MGD, Carvalho CWPD, Garcia-Rojas EE (2019) Physicochemical, thermal and rheological properties of synthesized carboxymethyl tara gum (caesalpinia spinosa). Int J Biol Macromol 134:595–603
18. Lin QQ, Liang R, Zhong F, Ye AQ, Singh H (2018) Effect of degree of octenyl succinic anhydride (OSA) substitution on the digestion of emulsions and the bioaccessibility of β-carotene in OSA-modified-starch-stabilized-emulsions. Food Hydrocoll 84:303–312
19. Sweedman MC, Tizzotti MJ, Schäfer C, Gilbert RG (2013) Structure and physicochemical properties of octenyl succinic anhydride modified starches: a review. Carbohydr Polym 92:905–920
20. Rossi B, Ponzini E, Merlini L, Grandori R, Galante YM (2017) Characterization of aerogels from chemo-enzymatically oxidized galactomannans as novel polymeric biomaterials. Eur Polym J 93:347–357
21. El-Thalouth IA, Rekaby M, Abdel-Rahman AH, El-Khabery SA (2012) Preparation and characterization of phosphorylated sesbania galactomannan gum derivatives and their applications in textile printing. Res J Text Appar 16:68–76
22. Tian J, Yin J, Tang X, Chen J, Luo X, Rao G (2013) Enhanced leaching process of a low-grade weathered crust elution-deposited rare earth ore with carboxymethyl sesbania gum. Hydrometallurgy 139:124–131
23. Wang Z, Zhu L, Zhang G, Zhao G, Zhu Y, Chang L (1997) Investigation of pyrolysis kinetics of carboxymethyl hydroxypropyl sesbania gum. J Therm Anal 49:1509–1512
24. Li H, Gao L, Xue M, Shen D, Cui Y (2012) Grafting modification of sesbania gum and its application to textile sizing. J Text Res 424:1211–1214
25. Tang H, Liu Y, Li Y, Li Q, Liu X (2020) Hydroxypropylation of cross-linked sesbania gum, characterization and properties. Int J Biol Macromol 152:1010–1019
26. Verma S, Ahuja M (2017) Carboxymethyl sesbania gum: synthesis, characterization and evaluation for drug delivery. Int J Biol Macromol 98:75–83
27. Tang HB, Wang L, Li YP, Dong SQ (2019) Effect of acidolysis and oxidation on structure and properties of konjac glucomannan. Int J Biol Macromol 130:378–387
28. Tang HB, Sun PX, Li YP, Dong SQ (2019) Esterification of sesbania gum hydrolysate in ionic liquid, optimization and characterization of its derivatives. Arab J Sci Eng 44:6381–6392
29. Abidin MN, Goh PS, Fauziismail A, Said N, Othman MHD, Hasbullah H, Kamal F (2018) Highly adsorptive oxidized starch nanoparticles for efficient urea removal. Carbohydr Polym 201:257–263
30. Li YT, Wang RS, Liang RH, Chen J, He XH, Chen RY, Liu W, Liu CM (2018) Dynamic high-pressure microfluidization assisting octenyl succinic anhydride modification of rice starch. Carbohydr Polym 193:336–342
31. Singh V, Ali SZ (2008) Properties of starches modified by different acids. Int J Food Prop 11:495–507

32. Srichuwong S, Isono N, Jiang H, Mishima T, Hisamatsu M (2012) Freeze-thaw stability of starches from different botanical sources: correlation with structural features. Carbohydr Polym 87:1275–1279
33. Wang S, Copeland L (2012) New insights into loss of swelling power and pasting profiles of acid hydrolyzed starch granules. Starch Stärke 64:538–544
34. Tang HB, Qu YF, Li YP, Dong SQ (2018) Surface modification mechanism of cross-linking and acetylation, and their influence on characteristics of high amylose corn starch. J Food Sci 83:1533–1541
35. Hazarika BJ, Sit N (2016) Effect of dual modification with hydroxypropylation and cross-linking on physicochemical properties of taro starch. Carbohydr Polym 140:269–278
36. Shi L, Cheng F, Zhu PX, Lin Y (2015) Physicochemical changes of maize starch treated by ball milling with limited water content. Starch - Stärke 67:772–779
37. Huhtamäki T, Tian XL, Korhonen JT, Ras RHA (2018) Surface-wetting characterization using contact-angle measurements. Nat Protoc 13:1521–1538
38. Zhang B, Wei BX, Hu XT, Jin ZY, Xu XM, Tian YQ (2015) Preparation and characterization of carboxymethyl starch microgel with different crosslinking densities. Carbohydr Polym 124:245–253
39. Xie WL, Shao L, Liu YW (2010) Synthesis of starch esters in ionic liquids. J Appl Polym Sci 116:218–224
40. Utrilla-Coello RG, Hernández-Jaimes C, Carrillo-Navas H, González F, Rodríguez E, Bello-Pérez LA, Alvarez-Ramirez J (2014) Acid hydrolysis of native corn starch: morphology, crystallinity, rheological and thermal properties. Carbohydr Polym 103:596–602
41. Qiu L, Shen Y, Wang T, Wang C (2018) Rheological and fracturing characteristics of a novel sulfonated hydroxypropyl guar gum. Int J Biol Macromol 117:974–982
42. Xu J, Zhou CW, Wang RZ, Yang L, Du SS, Wang FP, Ruan H, He GQ (2012) Lipase-coupling esterification of starch with octenyl succinic anhydride. Carbohydr Polym 87:2134–2144
43. Guo Z, Zhao B, Chen L, Zheng B (2019) Physicochemical properties and digestion of lotus seed starch under high-pressure homogenization. Nutrients 11:371–382
44. Altuna L, Herrera ML, Foresti ML (2018) Synthesis and characterization of octenyl succinic anhydride modified starches for food applications: a review of recent literature. Food Hydrocoll 80:97–110
45. Li D, Zhang X, Tian Y (2016) Ionic liquids as novel solvents for biosynthesis of octenyl succinic anhydride-modified waxy maize starch. Int J Biol Macromol 86:119–125
46. Hong Y, Li Z, Gu Z, Wang Y, Pang Y (2016) Structure and emulsification properties of octenyl succinic anhydride starch using acid-hydrolyzed method. Starch Stärke 69:1–9
47. Cai CH, Cai JW, Zhao LX, Wei CX (2014) In situ gelatinization of starch using hot stage microscopy. Food Sci Biotechnol 23:15–22
48. No J, Shin M (2019) Preparation and characteristics of octenyl succinic anhydride-modified partial waxy rice starches and encapsulated paprika pigment powder. Food Chem 295:466–474
49. Ma YS, Pan Y, Xie QT, Li XM, Zhang B, Chen HQ (2019) Evaluation studies on effects of pectin with different concentrations on the pasting, rheological and digestibility properties of corn starch. Food Chem 274:319–323
50. Lu X, Luo Z, Fu X, Xiao Z (2013) Two-step method of enzymatic synthesis of starch laurate in ionic liquids. J Agric Food Chem 61:9882–9891
51. Xie W, Wang Y (2011) Synthesis of high fatty acid starch esters with 1-butyl-3-methylimidazolium chloride as a reaction medium. Starch Stärke 63:190–197
52. Rajan A, Prasad VS, Abraham TE (2006) Enzymatic esterification of starch using recovered coconut oil. Int J Biol Macromol 39:265–272
53. Chooprayoon P, Boochathum P (2019) Self-crosslinkable hydroxylated natural rubber/carboxymethyl starch blend and its properties. Appl Polym 136:47271–47280
54. Fang JM, Fowler PA, Tomkinson J, Shill CA (2002) The preparation and characterisation of a series of chemically modified potato starches. Carbohydr Polym 47:245–252
55. No J, Mun S, Shin M (2019) Properties and digestibility of octenyl succinic anhydride-modified japonica-type waxy and non-waxy rice starches. Molecules 24:765–779
56. Leea S, Kima ST, Pant BR, Kwena HD, Song HH, Lee SK, Nehete SV (2010) Carboxymethylation of corn starch and characterization using asymmetrical flow field-flow fractionation coupled with multiangle light scattering. J Chromatogr A 1217:4623–4628
57. Luo Z, Zhou Z (2012) Homogeneous synthesis and characterization of starch acetates in ionic liquid without catalysts. Starch Stärke 64:37–44

58. Ren L, Dong Z, Jiang M, Tong J, Zhou J (2014) Hydrophobization of starch nanocrystals through esterification in green media. Ind Crops Prod 59:115–118
59. Yu ZY, Jiang SW, Zheng Z, Cao XM, Hou ZG, Xu JJ, Wang HL, Jiang ST, Pan LJ (2019) Preparation and properties of OSA-modified taro starches and their application for stabilizing pickering emulsions. Int J Biol Macromol 137:277–285